Designing Binary Electrocatalysts for Hydrogen Evolution in Saline Electrolyte Using Rapid Synthesis on Carbon Paper Supports

SCHOLARONE™
Manuscripts

Designing Binary Electrocatalysts for Hydrogen Evolution in Saline Electrolyte Using

Rapid Synthesis on Carbon Paper Supports

Connor S. Sullivan, Sangmin Jeong, Melissa E. King, Michael B. Ross*

Department of Chemistry, University of Massachusetts Lowell, Lowell, MA 01854

Abstract

Generating hydrogen from brackish or seawater could enable flexible energy generation, de-centralized electricity storage, and decreased reliance on energy-intensive water purification for hydrogen evolution reaction (HER). Platinum is often the most effective electrocatalyst for HER, however it is not as stable or efficient in nonideal electrolytes, such as seawater or non-acidic media. In this work, we investigate the activity and stability of binary electrocatalysts in a brackish neutral electrolyte. Using a rapid carbon-paper-based electrochemical synthesis method, we systematically assessed 45 unary and binary electrocatalysts. Four standout binary electrocatalyst materials were identified that showed either comparable or superior activity and stability to Pt in saline-containing electrolyte. Most notably, the 1Ni:1Pt electrocatalyst had a similar overpotential (60 mV) to a Pt control (50 mV), but with greater stability. Finally, we show that this carbon-paper-based synthesis method is scalable for synthesizing and assessing electrocatalysts. This work provides important insight both for rapid synthesis and comparison of new electrocatalysts, but also for the specific goal of performing HER in non-ideal aqueous conditions.

Introduction

The hydrogen evolution reaction (HER) is a key process for the storage of clean electricity and the synthesis of dihydrogen (H_2).[1-4] Mechanistically, this reaction involves the splitting of water molecules electrochemically and it is typically catalyzed by precious metal-based materials.[5-8] However, the high cost and limited availability of these materials and the need for high-grade water free of impurities pose significant challenges for large-scale deployment of water-splitting technologies.[1, 2, 7]

One promising alternative is to use non-precious metal electrocatalysts for HER, as opposed to the standout material Pt.[7] Non-precious metal electrocatalysts have emerged as promising alternatives for HER due to their low cost, abundance, and potential for high activity.[9-15] In recent years, significant progress has been made in developing efficient and stable non-precious metal electrocatalysts for HER in acidic and alkaline conditions.[16, 17] However, these electrocatalysts have not been extensively tested in the challenging conditions of low-grade water sources, such as seawater, which presents a highly complex corrosive environment. One possible solution for the complex corrosive environment in low-grade water sources is to develop alloys that can remain stable during HER. These alloys include known electrocatalysts such as Ni, Fe, Co, and Mn.[1, 12, 18]

Ideally, HER could be performed using the abundant low-grade water sources that are more readily available.[1, 15] This could enable flexible energy storage in regions where pure water is scarce while enabling long-term storage of renewable-generated electricity using deep-sea wind and other decentralized sources.[19] However, using low-grade water sources during HER poses several challenges, including corrosive chloride, a neutral pH, and other metal impurities. Cl– in seawater can be corrosive to the cathode electrocatalyst under reductive conditions, reducing

surface area and destabilizing active sites over time.[20-22] The neutral pH is challenging due to reduced proton concentrations for reduction to H_2. Trace impurities, such as metal ions, can destabilize the electrocatalyst over extended use through the formation and deposition of solid oxides and hydroxides.[2, 23]

To synthesize HER electrocatalysts that operate in suboptimal water electrolytes, we sought to rapidly screen unary and binary electrocatalysts in a neutral seawater simulant. In this work, we aimed to identify efficient and stable mixed metal electrocatalysts for HER in seawater. A rapid electrochemical synthesis strategy on carbon paper was used to assess nine unary electrocatalyst metals (Ag, Au, Co, Cu, Fe, Ni, Pd, Pt, and Rh) and all binary 1:1 combinations of these elements (thirty-six combinations). A cyclic electrochemical cycling method was used to compare performance durability over time in neutral (1M phosphate buffer at pH 7) and seawater simulating (1M phosphate buffer with 0.5M sodium chloride solution at pH 7) electrolytes. Six standout electrocatalysts were further characterized by transmission electron microscopy and chronoamperometry, revealing longer duration stability trends and insight into the nanoscale structure. Importantly, this method was shown to scale approximately linearly in area and current density over a nine-fold geometric area increase.

Materials and Methods

Materials for metal electrocatalysts

The synthesis of metal nanoparticles requires silver nitrate (AgNO$_3$, 99.9995%, Thermo Fisher Scientific), hydrogen tetrachloroaurate (HAuCl$_4$, 99.99%, Thermo Fisher Scientific), nickel(ii) chloride hydrate (NiCl$_2$ • H$_2$O, 99.995%, Thermo Fisher Scientific), rhodium(iv) chloride hydrate (RhCl• H$_2$O , 99.99%, Thermo Fisher Scientific), iron(ii) chloride tetrahydrate (FeCl$_2$ • 2H$_2$O,

99%, Thermo Fisher Scientific), cobalt(ii) chloride hexahydrate ($CoCl_2 \cdot 6\,H_2O$, 99.998%, Thermo Fisher Scientific), copper(ii) chloride hydrate ($CuCl_2 \cdot H_2O$, 99.999%, Thermo Fisher Scientific), platinum(iv) chloride ($PtCl_4$, 99.99%, Thermo Fisher Scientific), and palladium(ii) chloride ($PdCl_2$, 99.9%, Thermo Fisher Scientific). All chemicals were used without further purification and all solutions were prepared with ethanol.

Materials for electrochemical catalysis

A two-cell setup was used for all electrochemical experiments. The electrodes used were carbon paper electrode (AvCarb MGL 190, FuelCell Store), a Ag/AgCl reference electrode (3M), and a platinum mesh counter. A Nafion membrane (117, FuelCell Store) was used for all electrochemical experiments. The electrolytes were made with sodium dihydrogen phosphate dihydrate ($NaH_2PO_4 \cdot 2H_2O$, 99%, Thermo Fisher Scientific), sodium hydrogen phosphate anhydrous ($NaHPO_4$, 99%, Thermo Fisher Scientific), and sodium chloride (NaCl, 99%, Thermo Fisher Scientific). All chemicals were used without further purification and all solutions were prepared with 18.2 MΩ-cm resistivity water.

Electron Microscopy

Samples for transmission electron microscopy (TEM) were prepared by grinding the active area of the carbon paper electrodes into a fine powder and then the fine powder was suspended in ~1.5 mL of ethanol. Next, the electrode solution was drop-cast onto Cu Carbon Type-B grids. TEM was performed using a Phillips CM12 operated at 120 kV and a JEOL JEM-2100Plus TEM/STEM operated at 200 kV.

X-ray Photoelectron Spectroscopy

Samples for X-ray photoelectron spectroscopy (XPS) were prepared by loading an additional 800

µL of metal salt solution onto carbon paper electrodes with a 1 cm^2 active area, allowing for at least 1 hr. of drying time between 200 µL of metal salt solution. XPS was performed using a PHI VersaProbe II.

Methods for synthesizing electrocatalysts

To synthesize nanostructured metal electrocatalysts, 10 mM solutions of the precursor metal salts were dissolved in ethanol.[5] Next, 100 µL of solution was dropcast onto a 1 cm^2 active area on a carbon paper electrode. For the binary electrocatalysts, 50 µL of each solution was dropped onto the active area to yield equimolar metal ratios. Once dropcast, the electrodes were allowed to dry for at least one hour. The carbon paper was immersed in 1 M phosphate buffer (pH 7) and the metal salts were reduced using chronoamperometry for 5 minutes at -1.4 V vs. Ag/AgCl.

A two-compartment H-cell, separated using a Nafion membrane where the cathodic side was filled with one of two electrolytes and the anodic side was filled with 0.1 M sulfuric acid, was used for all electrochemical experiments. A Pt counter electrode was used as an anode. Two electrolytes were compared, 1 M phosphate buffer (pH 7). and 1 M phosphate buffer with 0.5 M NaCl solution added (pH 7). A Pine Research WaveDriver 100 potentiostat was used in all experiments.

Results and Discussion

Carbon-paper-supported electrocatalysts were synthesized by dropcasting equivalent mole amounts of metal salts onto carbon paper supports and then electrochemically reduced in a neutral buffer under a constant potential of -1.4V vs. Ag/AgCl for five minutes (Methods, **Figure 1**). This rapid synthetic method was used to assess a total of 45 electrocatalyst materials (both unary and binary metallic combinations) in equimolar ratios. Once synthesized on the carbon paper support,

the metals were all tested in a 1M neutral phosphate buffer (control) and a seawater electrolyte simulant (saline). The saline condition is comprised of the control condition with 0.5M NaCl added. Their electrocatalyst performance for HER was compared for overpotential and stability (using a linear sweep voltammetry [LSV] cycling method) in control and saline electrolyte (**Figure 1 and Table S2**).
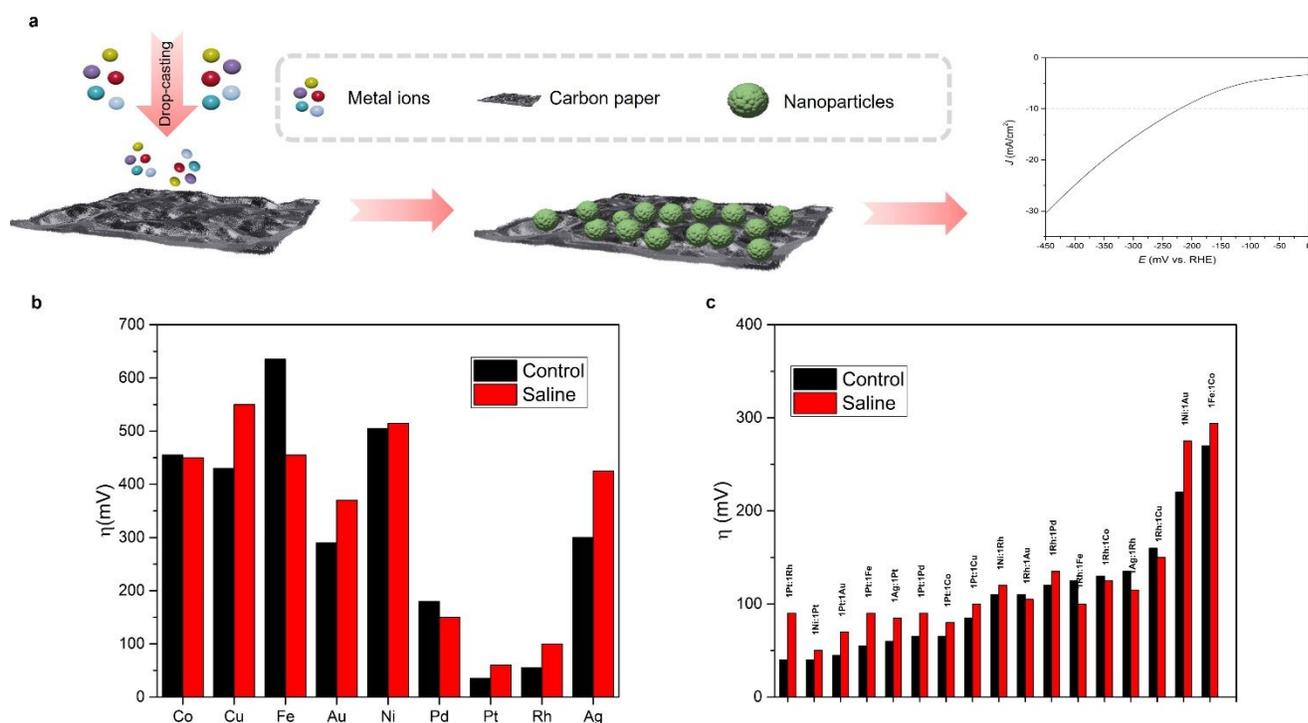

Figure 1. Metal electrocatalyst preparation, synthesis, and investigation of activity in a neutral saline electrolyte. (a) Scheme showing the metal salts being drop cast onto carbon paper supports and being synthesized at -1.4V in a neutral electrolyte. (b) Activities of unary metal electrocatalysts in saline and control electrolytes. (c) Activities of one-to-one binary electrocatalysts that achieved the best performance in saline and control electrolytes.

To begin this systematic analysis, nine unary electrocatalysts (Ag, Au, Co, Cu, Fe, Ni, Pd, Pt, and Rh) were first compared and tested using LSV (**Figure 1b**). As expected, these results show that platinum and rhodium achieved the lowest overpotentials in both electrolytes. However, one interesting observation was that iron performed better in the seawater-simulating electrolyte compared to its performance in the neutral electrolyte (**Figure 1b**). This can be explained by known electrocatalytic properties of Fe in neutral media. These properties include facilitating charge transport and creating phase boundaries which increase electroactive sites.[1, 18, 24] The worst performing metals in both electrolytes were those containing copper, cobalt, iron, and nickel.

After testing each individual metal, all thirty-six 1:1 binary combinations were assessed. Based on these results, all of the platinum and rhodium containing binary electrocatalysts achieved the lowest overpotential in both electrolytes. By combining platinum and rhodium with other metal electrocatalysts, stable binary electrocatalysts were synthesized. These binary electrocatalysts attained overpotentials that rivaled the single metal platinum and rhodium electrocatalyst but used half as much platinum and rhodium.

After determining the overpotential for each binary combination, the stability of each electrocatalyst was assessed in the same conditions. This was done by performing 150 polarizations in an automatic cycling process to simulate degradation over time. Once these curves were completed, the change in overpotential from the initial to final LSV was quantified. Through this method, we were able to see the effects of saline containing electrolyte on the electrocatalysts. On average, a 16 mV and 6 % degradation in overpotential was observed during cycling. Notably, the two nickel containing standout combinations showed good stability in both the control and saline electrolytes (**SI Figure 1**).

Through this systematic testing, electrocatalysts were narrowed down to a set of six standouts for structural investigation: Pt, Rh, Ni:Pt, Ni:Rh, Fe:Co, and Ni:Au. These standouts were chosen based on their low overpotentials in both electrolytes and/or if they improved in overpotential as a combination compared to their unary counterparts. To understand and compare the nanoscale structure of the synthesized electrodes, high-resolution transmission electron microscopy (HR-TEM), X-ray photoelectron spectroscopy (XPS), and energy-dispersive X-ray spectroscopy (EDS) were used. For TEM, the C-paper electrode was ground in a mortar and pestle, dispersed in ethanol, and imaged on a TEM grid. **Figure 2** shows TEM micrographs of the six standout electrocatalysts. Overall, the electrochemical synthesis method yielded ~5 nm metallic nanoparticles dispersed across a C support. The nanoparticles do not show significant aggregation and are generally of similar shape and morphology, suggesting that the synthetic method generates supported nanoparticles that are comparable for a variety of compositions.
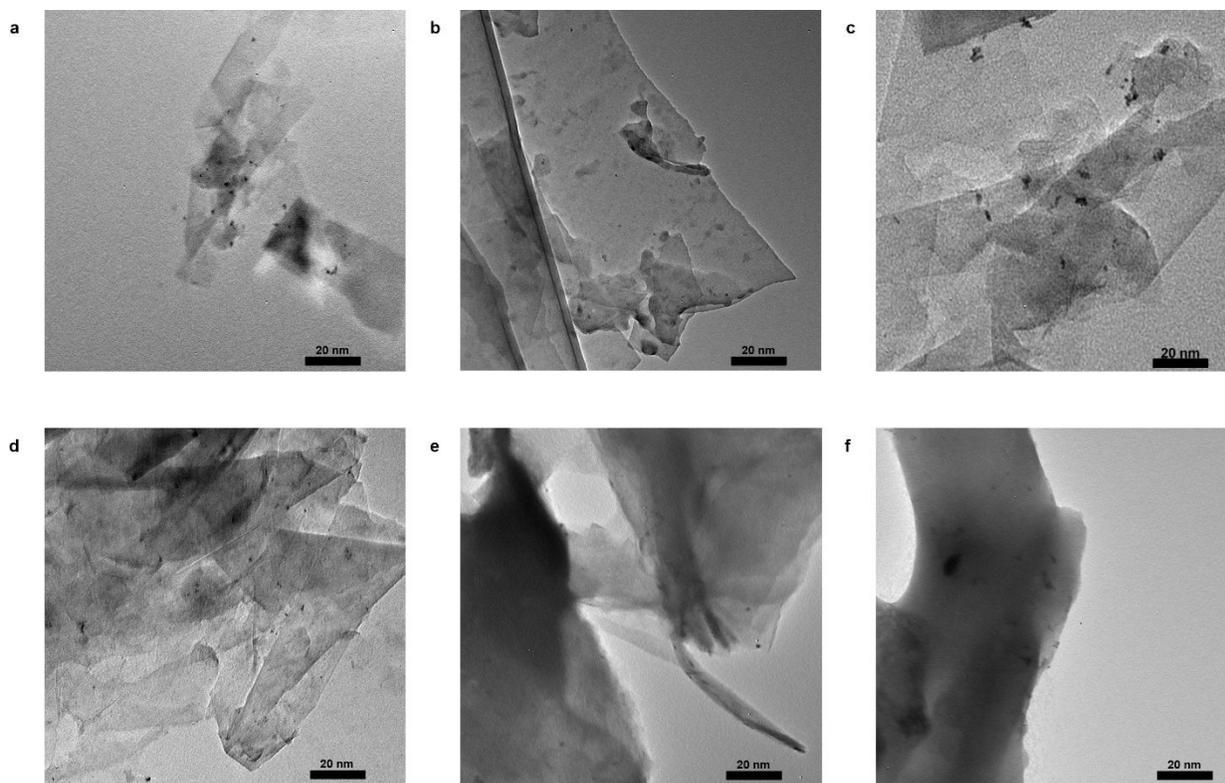
Figure 2. Transmission electron microscopy (TEM) of electrocatalysts. Micrographs of electrocatalysts composed of a) Pt b) Rh c) Ni:Pt d) Ni:Rh e) Ni:Au, and f) Fe:Co.

To further investigate the six standout electrocatalysts, a more rigorous quantitative analysis was performed. To achieve this, HR-TEM, XPS, and EDS were used to quantify the elemental distribution and composition of each electrocatalyst (**SI Figures 3- 5, Table S4**). From Figures 2 and 3, a size distribution of approximately 3-8 nm can be seen. Furthermore, the crystallinity of the metal electrocatalysts can be observed in Figures 3b and S3.
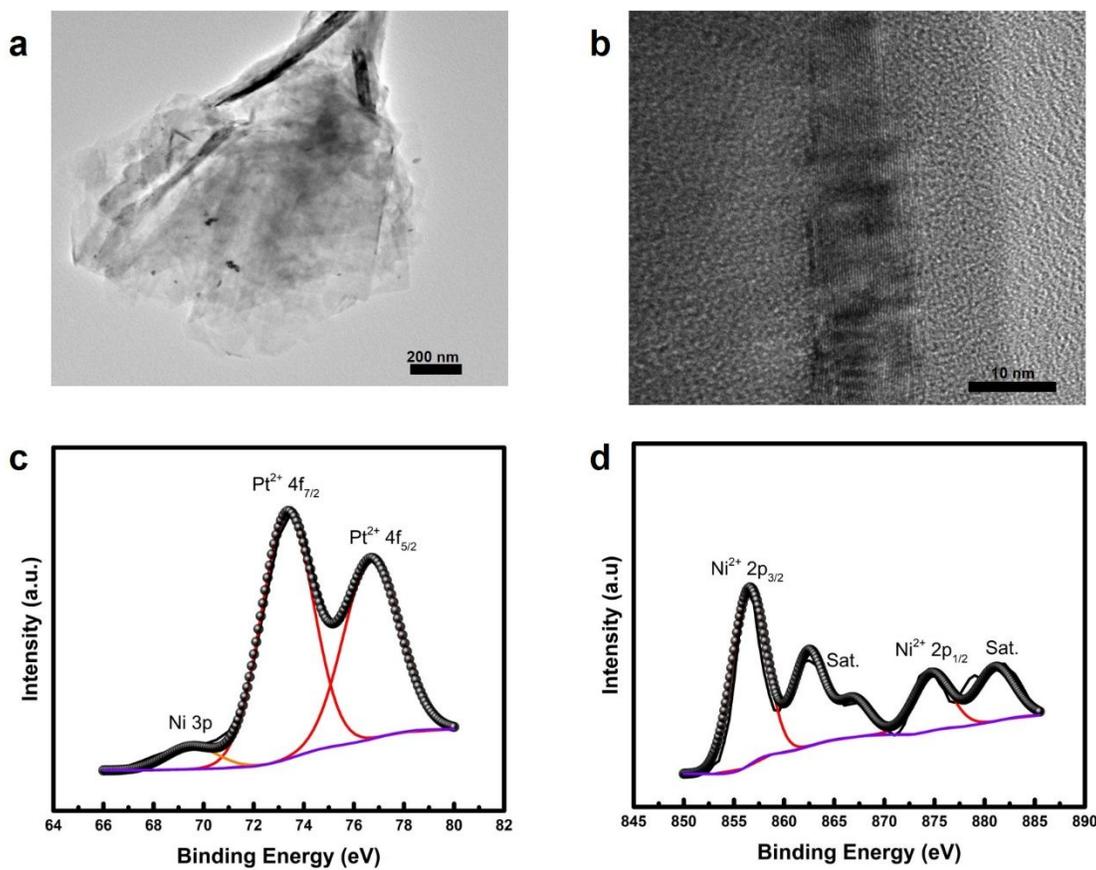
Figure 3. Quantitative analysis of Ni:Pt electrocatalyst. (a,b) High-resolution transmission electron microscopy images of Ni:Pt showing a magnification of and respectively. (c,d) High-resolution XPS scans of the characteristic Nickel and Platinum peaks on the Ni:Pt electrode.

Through XPS analysis the surface composition can be measured. Here, the Pt 4f core level spectrum (**Figure 3c**) clearly shows Pt^{4+} $4f_{7/2}$ (73.3 eV) and Pt^{4+} $4f_{5/2}$ (76.7 eV).[25] **Figure 3d** shows the resolved peaks in the Ni 2p core level spectra with two predominant peaks derived from Ni^{2+} (856.7 and 875.2 eV) and two satellite peaks at ~862 and ~881 eV.[26] The Pt:Ni atomic ratio derived from XPS data is 40:60 (**Table S4**). From these peak locations and the atomic ratios found in SI Table 4, the metal electrocatalysts have been uniformly distributed and nucleated on the surface of carbon paper support.

With better structural and compositional understanding in hand, we now focused on better quantifying their electrocatalytic activity. The platinum and rhodium electrocatalysts are the most efficient unary metal electrocatalysts with the lowest overpotentials. However, by cycling and comparison with saline electrolyte, the degradation over time can decrease their activity such that they are lower than many of their binary counterparts. Specifically, many of the binary combinations had overpotentials within 50-100 mV to start, while ending with overpotentials ~20-50 mV worse over time. While too numerous to list here, all of the relevant overpotentials can be found in **SI Table 3**. As such, we focused on a more systematic evaluation of the six standout electrocatalysts which had good performance and stability.
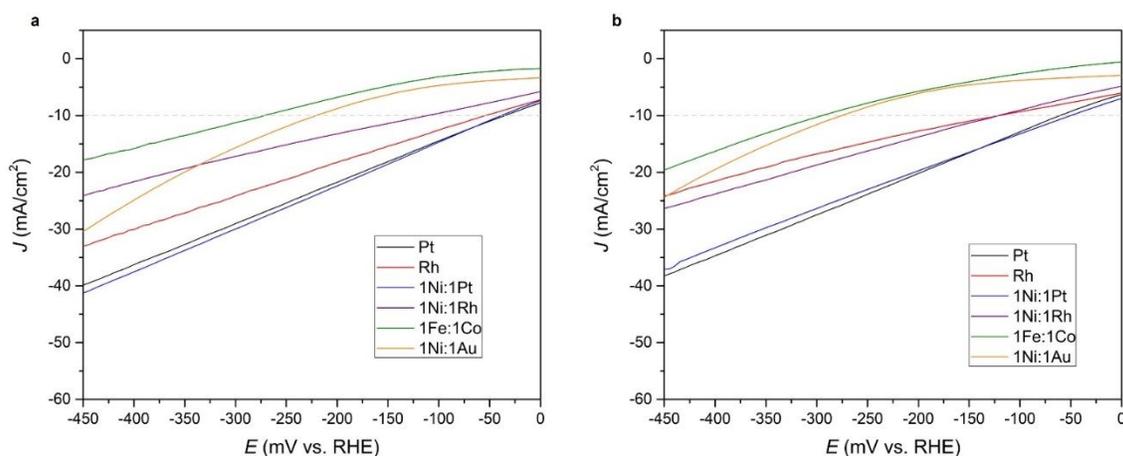
Figure 4: Polarization curves of six standout metal electrocatalysts. (a,b) HER polarization curves of standout metal electrocatalysts in neutral and saline electrolyte, respectively, at a sweep rate of 20 mV/s. The 6 electrocatalysts assessed were Pt, Rh, Ni:Pt, Ni:Rh, Fe:Co, and Ni:Au.

The Fe:Co was the best binary electrocatalyst that did not contain platinum, rhodium, or another noble metal. From the polarization curves in **Figure 4**, we see that Fe:Co had

overpotentials of 270 mV and 294 mV in the control and saline electrolytes, respectively. In both

electrolytes, Fe:Co only had a 20 mV and 25 mv drop in overpotential after 150 linear sweeps.

Fe:Co also showed a great improvement in performance and stability compared to the two unary

metal electrocatalysts that were used to form this combination (**SI Tables 1 and 2**), motivating

further investigation. By systematically analyzing the wide range of unary and binary

electrocatalysts many interesting combinations and alloys were discovered. These alloys have the

potential to have greater stability in HER with seawater conditions.[27]

All three nickel containing standouts showed great stability and performance in both the

control and saline condition. These results are supported since nickel is known to increase

corrosion resistance and long-term stability in seawater simulated media.[1, 24, 28, 29] From **Figure**

4b, the performance of Ni:Pt and Ni:Rh both rivaled platinum and rhodium by themselves and

were not greatly affected by the saline condition. Both Ni:Pt and Ni:Rh only saw an approximately

10 mV degradation of overpotential between the control condition and saline condition. By

comparison, the Pt on carbon support degraded 25 mV and Rh on carbon support degraded 45 mV

under the same experimental conditions. These data suggest that by combining high performance

electrocatalysts, such as platinum and rhodium, with a very stable metal electrocatalyst in nickel,

more robust binary electrocatalysts can be made that are stable in the harsher halide environment.[1,

30, 31]

The most noteworthy example of Ni-enhanced stability was in the Ni:Pt binary

electrocatalysts (**Figure 5**). The Ni:Pt binary electrocatalyst showed better performance in the

saline condition. In **Figure 5a**, the Ni:Pt binary electrocatalyst had an overpotential of 50 mV in

the saline condition, while Pt on carbon had an overpotential of 60 mV. Ni:Pt is the only binary

combination that competed with Pt on carbon in overall overpotential in either the control or saline

electrolytes.

To better compare the stability of the Ni:Pt electrocatalyst with the Pt only electrocatalysts, a more systematic comparative stability experiment was performed. In addition to the LSV cycling approach, steady-state chronoamperometry was performed to measure current degradation over time (**Figure S2**). In both instances, Ni:Pt electrocatalyst showed comparable performance to Pt on carbon support in both electrolytes and was one of the most robust during the two stability experiments. As expected, the Pt on carbon support had an overpotential of 35 mV vs. RHE while the Ni:PT had a slightly greater overpotential of 40 mV vs. RHE (**Figure 5b**) during the control experiments. During the saline experiments, Ni:Pt was significantly more stable in the saline condition after the 150 linear sweep voltammetry experiments (**Figure 5c**) than Pt.

Both Pt on carbon and Ni:Pt had robust stability in the control condition. The overpotential of Pt on carbon only changed by 2.2 mV from the first polarization curve and the overpotential of Ni:Pt changed by 4.94 mV from the first polarization curve in the control condition. In the saline condition however, the overpotential of Pt on carbon changed by 30 mV and the overpotential of Ni:Pt changed by 10.8 mV (**Figure 5c**). When comparing the current at -0.79 V vs. RHE, the Pt electrocatalyst degraded ~15% over 8 hours, compared to ~0% or even slight enhancement in current in the Ni:Pt case (**Figure S2**). The combination of a comparable overpotential in both electrolytes to Pt on carbon and better stability in the saline condition make Ni:Pt the best multi-metallic electrocatalyst from this work.
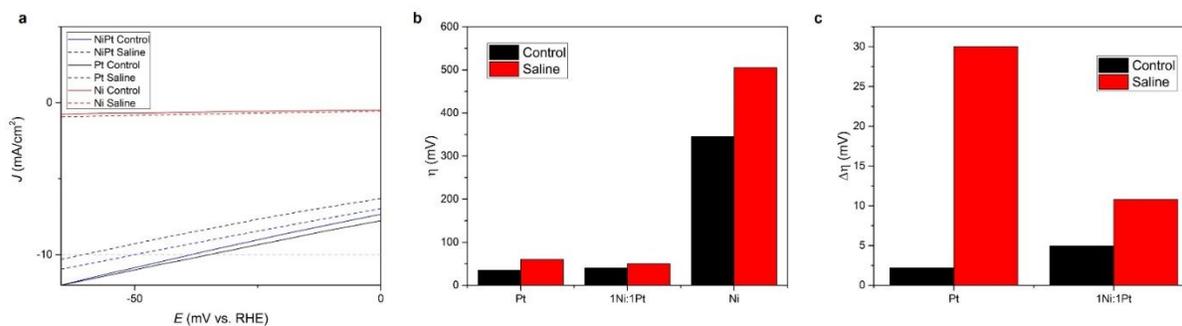
Figure 5. HER performance of Ni:Pt electrocatalysts on carbon paper support in both electrolyte solutions. (a) Polarization curves comparing the mixed Ni:Pt electrocatalyst to Pt and Ni with a sweep rate of 20 mV/s. (b) Corresponding overpotentials of Ni:Pt, Pt, and Ni. (c) Change in overpotentials of Ni:Pt and Pt electrocatalysts after 150 polarization cycles.

After the systematic analysis of the binary combinations, we sought to understand the scalability of this synthetic approach. All previous electrochemical experiments were done with a 1cm^2 active area and an equivalent one to one molar loading of metals. To assess the ability to scale, two larger electrodes were synthesized with 3cm^2 and 9cm^2 active area. These two electrodes, along with a 1cm^2 control electrode, were then loaded with 1- 3-, and 9-fold increases in the amount of metal ion precursor solution and dried overnight in a desiccator (**Figure 6a**). Once dried, Ni:Pt electrocatalysts were synthesized at a constant potential of -1.4V for five minutes using the same approach as described above (Methods, **Figure 1**). After synthesis, a linear sweep voltammetry experiment was performed with each electrode to compare the scalability of the current output (**Figure 6b**). In all instances, a clear 2.5-3-fold increase in the LSV was observed. To better assess the scalability as well as stability, steady-state chronoamperometry was performed to ensure robust stirring could remove bubbling at the surface and ensure sufficient mass transport is achieved.
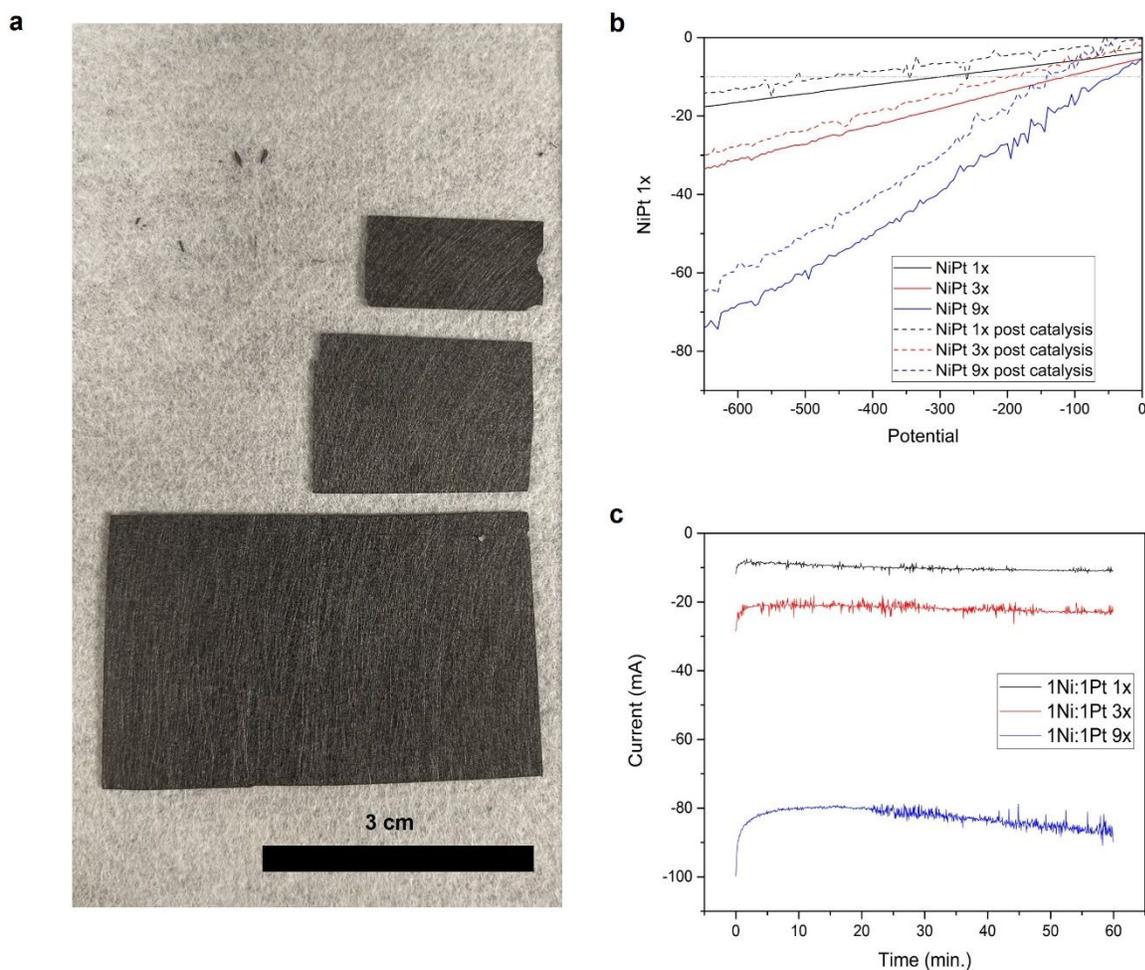
Figure 6. Scalable synthesis of Ni:Pt and its electrocatalytic performance. (a) Carbon paper electrode active areas increasing in scale from 1 cm^2 to 3 cm^2 to 9 cm^2. (b) LSV polarization curves of each electrode before and after chronoamperometry with a sweep rate of 20 mV/s. (c) Chronoamperometry of each electrode at -800 mV vs. Ag/AgCl for 1 hour.

Specifically, chronoamperometry was performed at -800 mV vs Ag/AgCl for 1 hour (**Figure 6c**). During this experiment, significant bubbling was observed at the surface of the electrode, leading to increased noise in the current. Overall, chronoamperometry shows an

approximately linear increase in current scaling with electrode area, with some increase in current over time (**Figure 6c**). Specifically, the 1 cm^2 area held an average current of ~8mA while the 3 cm^2 area held an average current of ~22 mA, a 2.75-fold increase. From 1 cm^2 to 9 cm^2, the current increases 10-fold from 8 mA (1 cm^2) to 80 mA (9 cm^2). After one hour of electrolysis, LSVs were performed again the activity was reduced by about 12% in each instance (**Figure 6b**).

Conclusion

Through a systematic analytical approach, our study has demonstrated the feasibility of using combinations of non-precious metals with noble metals for HER in neutral and halide-containing electrolytes. We have identified a Ni:Pt multi-metal electrocatalyst that exhibits competitive HER activity, comparable to that of platinum, with enhanced stability in the saline electrolyte simulant. Specifically, The Ni:Pt multi-metal electrocatalyst demonstrated a overpotential of 50 mV compared to the 60 mV over potential of pure Pt in the saline condition, indicating its superior catalytic activity. Additionally, the electrocatalysts maintained a high HER performance and showed excellent stability over extended periods of operation, indicating its robustness and corrosion resistance. In most instances, we found that Ni-containing electrocatalysts showed enhanced resistance to corrosion at the cathode as evidenced by stable or even enhanced overpotentials when compared to their unary counterparts.

Our findings open a promising avenue for the development of sustainable and cost-effective HER electrocatalysts that can withstand the harsh conditions of seawater. The use of non-precious metals such as nickel, which is abundant and inexpensive, can reduce the cost of HER and make it a more viable option for large-scale deployment. Furthermore, we have demonstrated the scalability of our method and the potential for generating clean hydrogen on a larger scale from

brackish water sources. This work introduces important questions relating to how alloy electrocatalysts can confer stability in challenging electrolytic conditions. Further experiments are needed to understand the exact mechanisms by how certain metals provide corrosion resistance and even enhanced overpotentials, potentially due to beneficial restructuring under bias.

Overall, our work highlights the potential of binary electrocatalysts for HER in seawater and provides valuable insights into the design and optimization of metal electrocatalysts for this application. Our findings contribute to the ongoing efforts towards the development of clean and sustainable energy production from seawater, which could have significant implications for the future of energy generation.

Author contributions

All authors contributed to the writing of this manuscript.

Declaration of interests

The authors declare no competing interests.

References

1.   Tong, W., et al., *Electrolysis of low-grade and saline surface water.* Nature Energy, 2020. **5**(5): p. 367-377.
2.   Dresp, S., et al., *Direct Electrolytic Splitting of Seawater: Opportunities and Challenges.* ACS Energy Letters, 2019. **4**(4): p. 933-942.
3.   Kucernak, A.R. and C. Zalitis, *General Models for the Electrochemical Hydrogen Oxidation and Hydrogen Evolution Reactions: Theoretical Derivation and Experimental Results under Near Mass-Transport Free Conditions.* The Journal of Physical Chemistry C, 2016. **120**(20): p. 10721-10745.
4.   Lokesh, S. and R. Srivastava, *Advanced Two-Dimensional Materials for Green Hydrogen Generation: Strategies toward Corrosion Resistance Seawater Electrolysis─Review and Future Perspectives.* Energy & Fuels, 2022. **36**(22): p. 13417-13450.
5.   Chen, P.-C., et al., *Heterostructured Au–Ir Catalysts for Enhanced Oxygen Evolution Reaction.* ACS Materials Letters, 2021. **3**(10): p. 1440-1447.
6.   Cheng, N., et al., *Platinum single-atom and cluster catalysis of the hydrogen evolution reaction.* Nature Communications, 2016. **7**(1): p. 13638.
7.   Hansen, J.N., et al., *Is There Anything Better than Pt for HER?* ACS Energy Letters, 2021. **6**(4): p. 1175-1180.
8.   Neufeld, O. and M.C. Toroker, *Platinum-Doped α-Fe2O3 for Enhanced Water Splitting Efficiency: A DFT+U Study.* The Journal of Physical Chemistry C, 2015. **119**(11): p. 5836-5847.
9.   King, L.A., et al., *A non-precious metal hydrogen catalyst in a commercial polymer electrolyte membrane electrolyser.* Nat Nanotechnol, 2019. **14**(11): p. 1071-1074.
10.   Dang, Y., et al., *RuO2-NiO Nanosheets on Conductive Nickel Foam for Reliable and Regeneratable Seawater Splitting.* ACS Applied Nano Materials, 2022. **5**(9): p. 13308-13318.
11.   Lv, Q., et al., *Featherlike NiCoP Holey Nanoarrys for Efficient and Stable Seawater Splitting.* ACS Applied Energy Materials, 2019. **2**(5): p. 3910-3917.
12.   Maarisetty, D., et al., *Tuning the Ni/Co Ratios and Surface Concentration of Reduced Molybdenum States for Enhanced Electrocatalytic Performance in Trimetallic Molybdates: OER, HER, and MOR Activity.* ACS Applied Energy Materials, 2022. **5**(11): p. 14059-14070.
13.   Pei, Y., et al., *Controlled Electrodeposition Synthesis of Co–Ni–P Film as a Flexible and Inexpensive Electrode for Efficient Overall Water Splitting.* ACS Applied Materials & Interfaces, 2017. **9**(37): p. 31887-31896.
14.   Popczun, E.J., et al., *Nanostructured Nickel Phosphide as an Electrocatalyst for the Hydrogen Evolution Reaction.* Journal of the American Chemical Society, 2013. **135**(25): p. 9267-9270.

15.   Song, S., et al., *One-Step Synthesis of Heterostructural MoS2-(FeNi)9S8 on Ni–Fe Foam Synergistically Boosting for Efficient Fresh/Seawater Electrolysis.* ACS Applied Energy Materials, 2022. **5**(2): p. 1810-1821.

16.   Zhou, Z., et al., *Electrocatalytic hydrogen evolution under neutral pH conditions: current understandings, recent advances, and future prospects.* Energy & Environmental Science, 2020. **13**(10): p. 3185-3206.

17.   Wang, L., et al., *Electronic Modulation of Metal–Organic Frameworks by Interfacial Bridging for Efficient pH-Universal Hydrogen Evolution.* Advanced Functional Materials, 2023. **33**(1): p. 2210322.

18.   Xiao, C., et al., *Improvement of the electrocatalytic performance of FeP in neutral electrolytes with Fe nanoparticles.* Chemical Engineering Journal, 2021. **408**: p. 127330.

19.   Vesborg, P.C.K., B. Seger, and I. Chorkendorff, *Recent Development in Hydrogen Evolution Reaction Catalysts and Their Practical Implementation.* The Journal of Physical Chemistry Letters, 2015. **6**(6): p. 951-957.

20.   Ke, S.-C., et al., *Mini Review on Electrocatalyst Design for Seawater Splitting: Recent Progress and Perspectives.* Energy & Fuels, 2021. **35**(16): p. 12948-12956.

21.   Zhang, P., et al., *Direct Electrochemical Seawater Splitting for Green Hydrogen and Artificial Reefs.* ACS Applied Energy Materials, 2023. **6**(14): p. 7636-7642.

22.   Kumaravel, V. and A. Abdel-Wahab, *A Short Review on Hydrogen, Biofuel, and Electricity Production Using Seawater as a Medium.* Energy & Fuels, 2018. **32**(6): p. 6423-6437.

23.   Chang, J. and Y. Yang, *Advancements in Seawater Electrolysis: Progressing from Fundamental Research to Applied Electrolyzer Application.* Renewables, 2023. **1**(4): p. 415-454.

24.   Song, L.J. and H.M. Meng, *Effect of carbon content on Ni–Fe–C electrodes for hydrogen evolution reaction in seawater.* International Journal of Hydrogen Energy, 2010. **35**(19): p. 10060-10066.

25.   Peuckert, M., F.P. Coenen, and H.P. Bonzel, *XPS study of the electrochemical surface oxidation of Platinum in N H2SO4 acid electrolyte.* Electrochimica Acta, 1984. **29**(10): p. 1305-1314.

26.   Bagus, P.S., et al., *Main and Satellite Features in the Ni 2p XPS of NiO.* Inorganic Chemistry, 2022. **61**(45): p. 18077-18094.

27.   Wu, L., et al., *Electrochemical performance of porous Ni-alloy electrodes for hydrogen evolution reaction from seawater electrolysis.* RSC Advances, 2020. **10**(73): p. 44933-44945.

28.   Miao, J., et al., *Hierarchical Ni-Mo-S nanosheets on carbon fiber cloth: A flexible electrode for efficient hydrogen generation in neutral electrolyte.* Science Advances, 2015. **1**(7): p. e1500259.

29.   Zhao, Y., et al., *Interfacial nickel nitride/sulfide as a bifunctional electrode for highly efficient overall water/seawater electrolysis.* Journal of Materials Chemistry A, 2019. **7**(14): p. 8117-8121.

30.   Wang, Q., et al., *Synthesis and Design of a Highly Stable Platinum Nickel Electrocatalyst for the Oxygen Reduction Reaction.* ACS Applied Materials & Interfaces, 2021. **13**(44): p. 52681-52687.

31.   Qian, X., et al., *Decoration of Micro-/Nanoscale Noble Metal Particles on 3D Porous Nickel Using Electrodeposition Technique as Electrocatalyst for Hydrogen Evolution*

Reaction in Alkaline Electrolyte. ACS Applied Materials & Interfaces, 2015. **7**(29): p. 15716-15725.